4-2016

Disentangling greenhouse warming and aerosol cooling to reveal Earth's climate sensitivity

T. Storelvmo
Yale University

T. Leirvik
University of Nordland

U. Lohmann
ETH-Zurich

Peter C. B. PHILLIPS
Singapore Management University, peterphillips@smu.edu.sg

M. Wild
ETH-Zurich

Citation

Disentangling Greenhouse Warming and Aerosol Cooling to Reveal Earth's Transient Climate Sensitivity

Authors: T. Storelvmo[1*], T. Leirvik[2], U. Lohmann[3], P. C. B. Phillips[1], M. Wild[3]

[1] Yale University, New Haven, CT, USA.
[2] University of Nordland, Bodø, Norway.
[3] ETH-Zurich, Zurich, Switzerland.

Earth's climate sensitivity has been the subject of heated debate for decades, and recently spurred renewed interest after the latest IPCC assessment report suggested a downward adjustment of the most likely range of climate sensitivities (1). Here, we present an observation-based study based on the time period 1964 to 2010, which is unique in that it does not rely on global climate models (GCMs) in any way. The study uses surface observations of temperature and incoming solar radiation from approximately 1300 surface sites, along with observations of the equivalent CO_2 concentration ($CO_{2,eq}$) in the atmosphere, to produce a new best estimate for the transient climate sensitivity of 1.9K (95% confidence interval 1.2K – 2.7K). This is higher than other recent observation-based estimates (2, 3), and is better aligned with the estimate of 1.8K and range (1.1K – 2.5K) derived from the latest generation of GCMs. The new estimate is produced by incorporating the observations in an energy balance framework, and by applying statistical methods that are standard in the field of Econometrics, but less common in climate studies. The study further suggests that about a third of the continental warming due to increasing $CO_{2,eq}$ was masked by aerosol cooling during the time period studied.

Atmospheric CO_2 concentration is projected to double from preindustrial levels during this century (4), and constraining Earth's temperature response is a primary objective for designing mitigation and adaptation policies (5). While substantial attention has been devoted to model estimates of Earth's equilibrium climate sensitivity (6) (i.e., the temperature response to CO_2 doubling once a new equilibrium climate state is reached over several thousand years (7)), more relevant to public and policy makers is the temperature change that occurs at the time of CO_2 doubling, known as 'transient climate sensitivity' (TCS). Constraining TCS based on observational records is complicated by the fact that recent climate change was not forced by CO_2 changes alone. Downward solar radiation at the surface (DSRS, measured in Wm^{-2}) reported at approximately 1300 surface stations over the time period 1964 -2010 (Fig. 1a) from 1964 to 2010 (Fig. 1b) display a downward trend in DSRS which is commonly referred to as 'global dimming' *(8)*. The most plausible explanation for global dimming is increased atmospheric aerosol loading derived from anthropogenic burning of fossil fuels and biomass. The overall effect of aerosols increases Earth's albedo, either by direct interaction with solar radiation, or by increasing the lifetime,

areal extent, and/or reflectivity of clouds (9). For some portions of the world, the appearance of regional trends opposing the global negative DSRS trend (i.e., regional brightening) is observed towards the end of the 20th century, consistent with a reduction in aerosol emissions in much of the developed world (8). Atmospheric aerosol loading is broadly reflected in global emissions of sulfur dioxide (SO_2), a precursor for sulfate aerosols (Fig.1b). Sulfate is only one of several aerosol species emitted by human activity, but the relationship between SO_2 emissions and downward solar radiation broadly reflects the impact of anthropogenic atmospheric aerosol loading on global dimming, and thereafter on the somewhat weaker patterns of regional brightening. Note that trends in volcanic activity or insolation would also affect DSRS, and that similar emissions may have different radiative effects depending on factors like latitude and climate regime (10).

Perturbations to Earth's radiation budget, whether by greenhouse gases or aerosols, are commonly referred to as radiative forcings (RFs, Wm^{-2}). Positive RFs exerted by anthropogenic CO_2, imply a net energy gain by the Earth-atmosphere system and subsequent warming, while negative RFs exerted by anthropogenic aerosols, imply net energy loss.

TCS relates the net RF (ΔF) to the change in global mean temperature (ΔT) through the following equation:

$$TCS = \frac{F_{2x}\Delta T}{\Delta F} \qquad\qquad\qquad (1)$$

where F_{2X} is the forcing due to a doubling of atmospheric CO_2 concentrations. Over the last century, the net forcing has been dominated by the two competing RFs due to long-lived greenhouse gases (GHGs) and aerosols ($\Delta F \approx \Delta F_{GHG} + \Delta F_{AER}$) (11). For an observed temperature change, an overestimation of ΔF translates into an underestimation of the *TCS* (Eq. 1), and vice versa (12). Compared to the RF resulting from GHG increases, the RF associated with aerosol forcing is poorly constrained. While tremendous progress has been made on the representation of various aerosol processes in GCMs, aerosol-cloud interactions remain a major source of uncertainty (21), and the spread in GCM estimates of cloud-mediated and total aerosol effects on climate is almost as wide today as when the field emerged two decades ago (13). Because of the intimate coupling between the uncertain ΔF and TCS (14), estimates of the TCS simulated by GCMs are considered unreliable. TCS estimates that are independent of GCMs are critical for advancing the topic.

For this study, we estimate TCS by applying surface air temperature observations from the high-resolution (0.5°) data set from the Climate Research Unit (CRU) (15), equivalent CO_2 concentrations ($CO_{2,eq}$) from the Annual Greenhouse Gas Index (AGGI) (16) and DSRS from the Global Energy Balance

Archive (GEBA) (17). Observations from the ~1300 surface stations considered were used to estimate the free parameters of a set of equations predicting temperature at individual stations as a function of $CO_{2,eq}$ and SRDS, using a so-called 'Dynamic Panel Data Method' (18)). Using this framework, the observed temperature evolution from 1964 to 2010 can be reasonably reproduced, and yields a spatially averaged temperature increase of approximately 0.8K (Fig. 3). Furthermore, a calculation of temperature evolution under the hypothetical case that $CO_{2,eq}$ remained constant at 1964 values results in a cooling that reflects the total aerosol effect. Surface cooling is approximately 0.4K averaged over the surface stations considered. Conversely, if DSRS is kept constant at 1964 levels, corresponding to constant atmospheric aerosol concentrations, a warming of 1.2K is calculated. In other words, about one third of potential continental warming attributable to increased greenhouse gas concentrations has been masked by aerosol cooling during this time period. The masking effect is strongest before 1990, consistent with previous studies for that time period (19).

The analysis also yields a best estimate of the TCS of 3.0K for land, with a 95% confidence interval of 1.8 – 4.2K, which is obtained by computing $\gamma_3 \log 2$ where γ_3 is the parameter in Eq. 2 that controls the sensitivity to $CO_{2,eq.}$ Given that land has warmed at exactly double the rate of the ocean over the past century, TCS for the entire globe is estimated to be ~1.9K (95% confidence interval 1.2 – 2.7˚K) (obtained by taking $TCS_{Globe} \approx TCS_{Land}(f_{Land}+0.5f_{Ocean})$, where f_{Ocean} and f_{Land} refer to the global land/ocean fractions). A recent analysis used energy budget calculations combined with observations to constrain climate sensitivity (2), but required GCMs for information on radiative forcings. That study reported a 95% confidence interval for TCS based on the time period 1970-2009 of 0.7-2.5K, and a best estimate of 1.4K. Our GCM-independent method yields a best estimate that is 0.5K higher, and uncomfortably close to the amount of warming that more than 100 countries have adopted as a limit beyond which dangerous climate change is thought to ensue.

The hiatus in global warming observed over the last decade has been the topic of numerous papers in recent years, and its cause is currently being debated (20-22). Some recent estimates of climate sensitivity that incorporate the most up-to-date observational data sets, including the apparent global warming hiatus, have reported very low climate sensitivities (3, 23). To test the sensitivity of our method to the period selected for analysis, we analyzed 25-year subsets of the time period 1964 to 2010, and produced probability density functions (PDFs) for TCS (Fig. 4). Independent of which 25-year time window is selected, the TCS for land lies in the interval 2-4.5K. The PDFs are relatively broad, with high TCSs typically stemming from 25-year periods of rapid warming and lower values during periods with weak temperature trends. Analyses based on shorter time windows are obviously more susceptible to climate variability, and therefore more likely to produce biased trends. Nevertheless, all three PDFs peak at a land TCS of 3-4K, increasing the confidence in the best estimate from the full 46-year time period.

Thus, the observational-based and GCM-independent analysis presented here supports the best TCS estimate and range produced by GCMs, despite incorporating observations from the so-called hiatus, which has caused other observational methods to produce anomalously low TCS estimates. The prevailing view is that the hiatus can be attributed to variability internal to the climate system, which temporarily causes more heat to mix into the deep ocean via the Equatorial Pacific (24). Thus, we suggest that studies that produce anomalously low climate sensitivities as a result of incorporating the hiatus period are overly sensitive to temperature trends of the past decade, and to climate variability in general.

Methods

This study relies on three observational datasets: The Global Energy Balance Archive (GEBA, www.geba.ethz.ch), the Climate Research Unit Time Series (CRU TS, version 3.2, badc.nerc.ac.uk/data/cru/) and the National Oceanic and Atmospheric Administration (NOAA) Annual Greenhouse Gas Index (AGGI, http://www.esrl.noaa.gov/gmd/aggi/) datasets. The GEBA dataset reports monthly mean downwelling shortwave radiation (SRDS) reaching the surface, as measured at approximately 2,500 instrumented surface stations worldwide. Out of these, data only from about 1,300 surface stations are selected for the purpose of this study, based on strict criteria on time series length and continuity, as well as data quality control. The availability of high-quality continuous data limited the time period studied here to 1964 – 2010. For each selected station, i, the annual mean time series of SRDS, denoted R_i, is assigned a corresponding high-resolution temperature time series T_i from CRU TS3.2. The CRU TS3.2 dataset is available for download from the British Atmospheric Data Center (BADC) and is provided on a 0.5x0.5 degree horizontal resolution. The third and final dataset, AGGI, provides annual and global mean atmospheric abundances for all major well-mixed long-lived greenhouse gases: carbon dioxide, methane, nitrous oxide, CFC-12 and CFC-11, as well as 15 minor halogenated gases from the NOAA global air sampling network. By converting the abundances of all other gases than CO_2 into CO_2 equivalent abundances, the AGGI data set can offer an annual and global mean time series of equivalent CO_2 abundance ($CO_{2,eq}$), which is the time series that is used here. Because these well-mixed GHGs exhibit little spatial variability, the global mean values can be taken as valid for all surface stations. These time series, two of them specific to each of the 1300 surface stations and the third offering one single annual value for the entire globe, are incorporated into Equations 1 and 2 below, which combined predict the temperature evolution at individual surface sites.

The equations thus describe the annual mean temperature at any given station in year $t+1$ as a function of local and global mean temperatures (T_i and T), local and global mean SRDS, as well as the global mean $CO_{2,eq}$, all for the previous year t. The dependence of local temperature evolution on these variables is

justified based on energy balance considerations, but note that we are not explicitly solving an energy balance model here. Instead, the energy balance framework is simply used to identify variables that might be expected to exert an influence on local temperature evolution. Thereafter, the parameters that relate local temperature evolution to these variables are determined entirely by our observed time series, using the following equations:

$$T_{i,t+1} = \beta_1 T_{i,t} + \beta_2 R_{i,t} + \lambda_t \qquad (1)$$

$$\lambda_t = \gamma_0 + \gamma_1 T_t + \gamma_2 R_t + \gamma_3 \log(CO_{2,eq}) \qquad (2)$$

where β_1, β_2, γ_0, γ_1, γ_2 and γ_3 are parameters that are constrained by the 3-dimentional datasets. This is done by the use of a so-called *Dynamic Panel Data Method (DPDM)*, which goal is to estimate the parameter values (the $\beta's$ and $\gamma's$) that best describe all observations in both time and space. Table 1 shows the parameter values that result from the application of the DPDM. Note that this method implicitly assumes that there is no long-term trend in Earth's heat capacity, which is dominated by ocean heat uptake.

As expected, at any year the present temperature will be a relatively good predictor of next year's temperature (parameter β_1). The temperature influence of the local DSRS is evident by the fact that β_2 is positive and significantly different from zero – the more incoming solar radiation at the surface, the warmer. The parameter that relates local temperature in year $t+1$ to the station mean temperature in year t (γ_1) represents two processes; transport of heat to/from the stations from/to the surroundings, as well as the Planck feedback (a warmer land surface loses more energy to space through infrared radiation). The observations suggest that the latter dominates. The parameter relating local temperature to global (that is, station-mean) DSRS (γ_2) is not significantly different from zero, and the observations therefore suggest that the global solar radiation balance does not have a strong influence on local temperature trends. Finally, $CO_{2,eq}$ has a strong impact on local temperatures, as evident by the positive γ_3 which is significantly different from zero.

Table 1: Parameter values, standard errors and confidence intervals for the parameters of Eqs. 1 and 2.

Parameter	Value	Std. Error	95% confidence interval	Relevant variable
β_1	0.9212	0.0040	(0.9133, 0.9292)	T_i
β_2	0.0127	0.0006	(0.0108, 0.0146)	R_i
γ_1	-0.8900	0.1568	(-1.2065, -0.5737)	T
γ_2	0.0002	0.0066	(-0.0131, 0.0136)	R
γ_3	4.3143	0.8705	(2.5588, 6.0699)	$CO_{2,eq}$

A)

B)
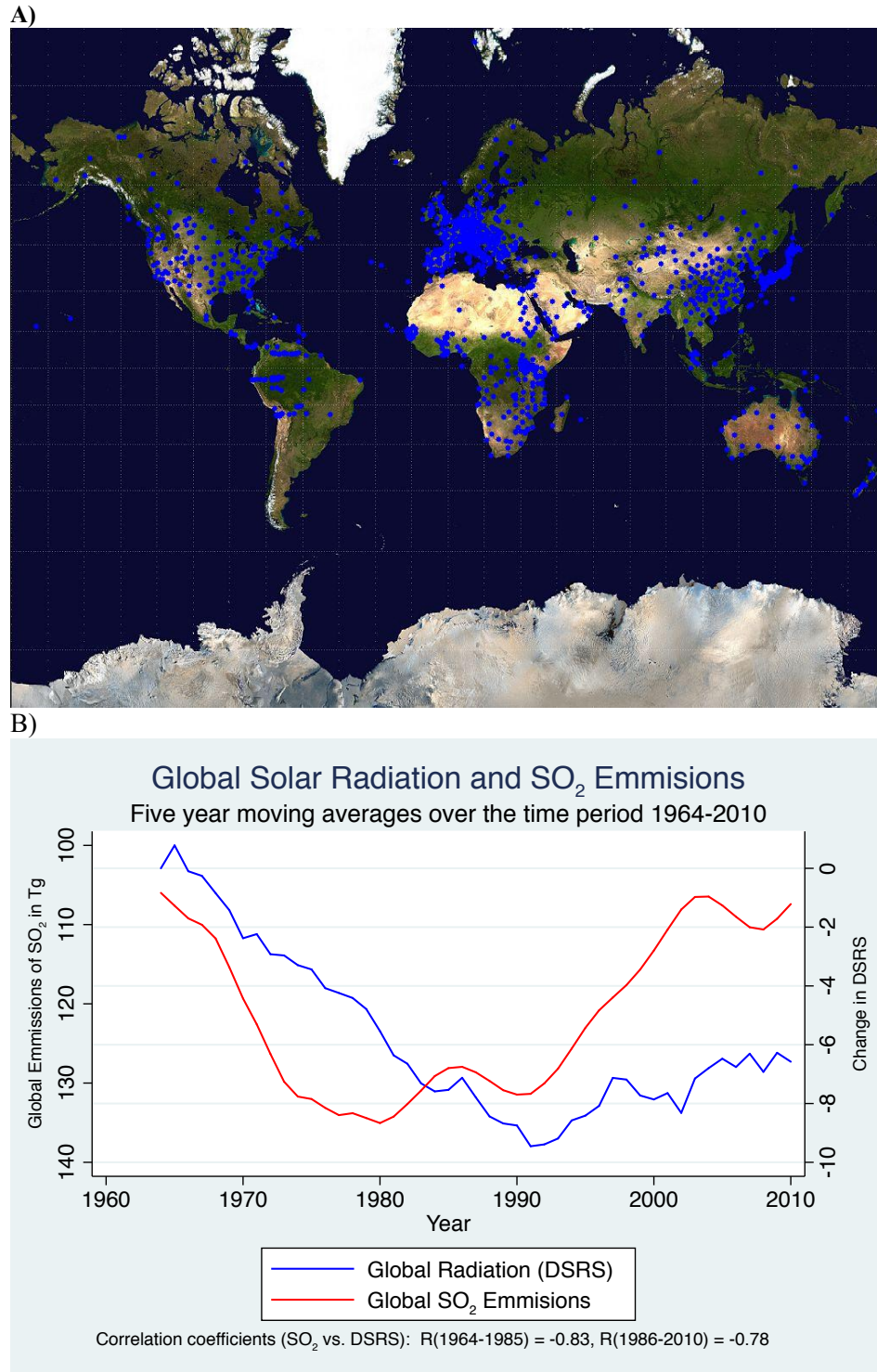
Fig. 1: Upper panel: Blue dots indicate the location of each of the ~1300 surface stations incorporated in the study. Lower panel: Trend in DSRS, shown as the change relative to 1964, calculated by averaging the year-to-year change over all stations displayed above (right axis, green curve). Also shown are global mean emissions of sulfur dioxide, SO_2 (blue curve, left axis, reversed) (25, 26), a precursor to sulfate aerosols. Both curves show 5-year running means.
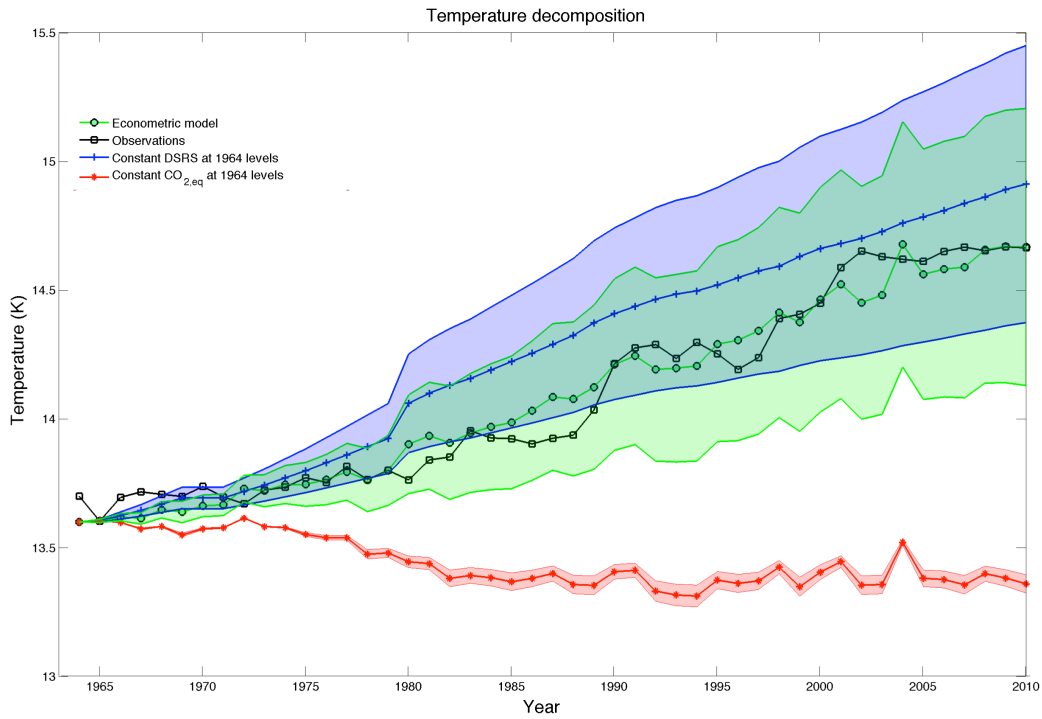
Fig. 3: Global land temperature as observed (black curve, CRU TS3.2 data sampled at GEBA stations only, displayed as 5-year running mean), and as predicted with Equations 1 and 2 (green curve). The red curve is calculated using the same framework, but setting $CO_{2,eq}$ concentrations constant at 1964 values, such that the temperature trend is controlled by the DSRS trend alone. Likewise the blue curve shows the temperature predicted with DSRS constant at 1964 values, such that the temperature trend is controlled only by $CO_{2,eq}$. Shadings represent the standard error.
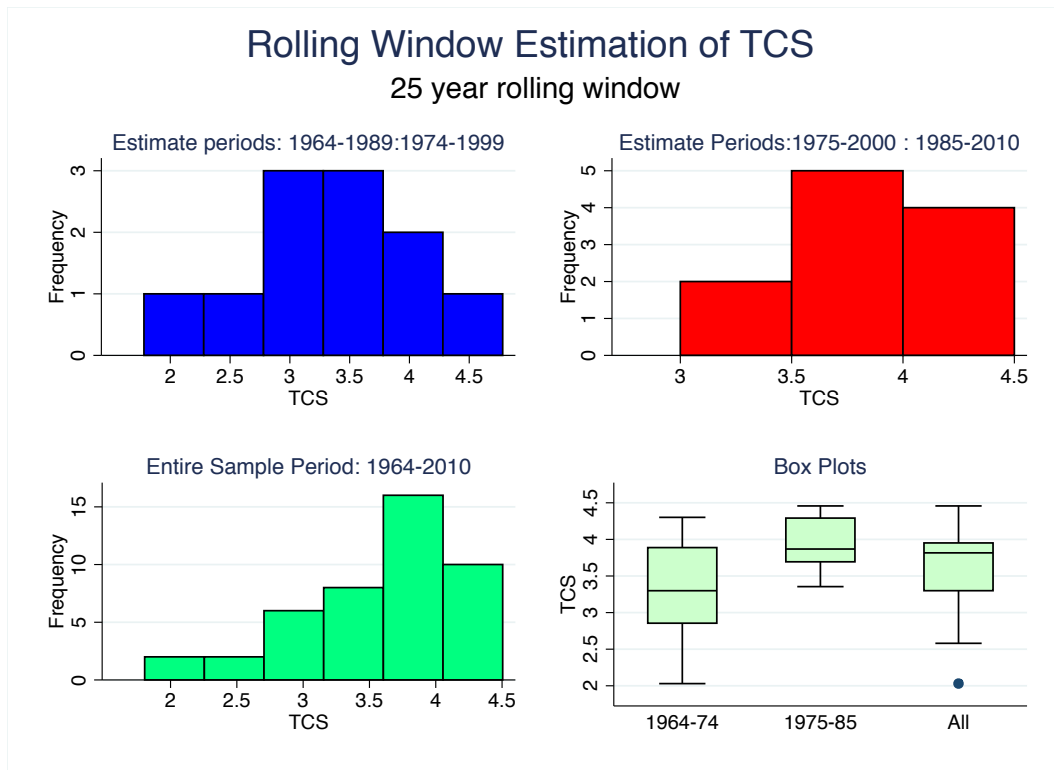
Fig. 4: TCS distributions calculated based on 25-year rolling windows: (A) For 25-year periods beginning in 1964-1974, (B) For 25-year periods beginning in 1975-1985, (C) For all 25-year periods of the 46-year record. Also shown (D) are the median (horizontal lines), 25th and 75th percentiles (boxes) and maximum/minimum values for all distributions (outliers marked with circles). Note that these TCS estimates are valid for land areas.

References:

1.   Flato G, J. Marotzke, B. Abiodun, P. Braconnot, S.C. Chou, W. Collins, P. Cox, F. Driouech, S. Emori, V. Eyring, C. Forest, P. Gleckler, E. Guilyardi, C. Jakob, V. Kattsov, C. Reason and M. Rummukainen (2013) Evaluation of Climate Models. *Climate Change 2013: The Physical Science Basis. Contribution of Working Group I to the Fifth Assessment Report of the Intergovernmental Panel on Climate Change*, ed Stocker TF, D. Qin, G.-K. Plattner, M. Tignor, S.K. Allen, J. Boschung, A. Nauels, Y. Xia, V. Bex and P.M. Midgley (Cambridge University Press, Cambridge, United Kingdom and New York, NY, USA), pp 741–866.
2.   Otto A*, et al.* (2013) Energy budget constraints on climate response. *Nat Geosci* 6(6):415-416.
3.   Lewis N & Curry J (2014) The implications for climate sensitivity of AR5 forcing and heat uptake estimates. *Clim Dynam*:1-15.
4.   Collins M, R. Knutti, J. Arblaster, J.-L. Dufresne, T. Fichefet, P. Friedlingstein, X. Gao, W.J. Gutowski, T. Johns, G. Krinner, M. Shongwe, C. Tebaldi, A.J. Weaver and M. Wehner (2013) Long-term Climate Change: Projections, Commitments and Irreversibility. *Climate Change 2013: The Physical Science Basis. Contribution of Working Group I to the Fifth Assessment Report of the Intergovernmental Panel on Climate Change*, ed Stocker TF, D. Qin, G.-K. Plattner, M. Tignor, S.K. Allen, J. Boschung, A. Nauels, Y. Xia, V. Bex and P.M. Midgley (Cambridge University Press, Cambridge, United Kingdom and New York, NY, USA), pp 1029–1136.
5.   Nordhaus WD (2010) Economic aspects of global warming in a post-Copenhagen environment. *P Natl Acad Sci USA* 107(26):11721-11726.
6.   Allen MR & Frame DJ (2007) Call Off the Quest. *Science* 318(5850):582-583.

7. Zeebe RE (2013) Time-dependent climate sensitivity and the legacy of anthropogenic greenhouse gas emissions. *P Natl Acad Sci USA* 110(34):13739-13744.
8. Wild M (2012) Enlightening Global Dimming and Brightening. *B Am Meteorol Soc* 93(1):27-37.
9. Koren I, Dagan G, & Altaratz O (2014) From aerosol-limited to invigoration of warm convective clouds. *Science* 344(6188):1143-1146.
10. Kühn T*, et al.* (2014) Climate impacts of changing aerosol emissions since 1996. *Geophys Res Lett* 41(13):4711-4718.
11. Myhre G, D. Shindell, F.-M. Bréon, W. Collins, J. Fuglestvedt, J. Huang, D. Koch, J.-F. Lamarque, D. Lee, B. Mendoza, T. Nakajima, A. Robock, G. Stephens, T. Takemura and H. Zhang (2013) Anthropogenic and Natural Radiative Forcing. *Climate Change 2013: The Physical Science Basis. Contribution of Working Group I to the Fifth Assessment Report of the Intergovernmental Panel on Climate Change*, ed Stocker TF, D. Qin, G.-K. Plattner, M. Tignor, S.K. Allen, J. Boschung, A. Nauels, Y. Xia, V. Bex and P.M. Midgley (Cambridge University Press, Cambridge, United Kingdom and New York, NY, USA), pp 659–740.
12. Andreae MO, Jones CD, & Cox PM (2005) Strong present-day aerosol cooling implies a hot future. *Nature* 435(7046):1187-1190.
13. Lohmann U*, et al.* (2010) Total aerosol effect: radiative forcing or radiative flux perturbation? *Atmos Chem Phys* 10(7):3235-3246.
14. Kiehl JT (2007) Twentieth century climate model response and climate sensitivity. *Geophys Res Lett* 34(22).
15. Harris I, Jones PD, Osborn TJ, & Lister DH (2014) Updated high-resolution grids of monthly climatic observations - the CRU TS3.10 Dataset. *Int J Climatol* 34(3):623-642.
16. Hofmann DJ*, et al.* (2006) The role of carbon dioxide in climate forcing from 1979 to 2004: introduction of the Annual Greenhouse Gas Index. *Tellus B* 58(5):614-619.
17. Gilgen H & Ohmura A (1999) The Global Energy Balance Archive. *B Am Meteorol Soc* 80(5):831-850.
18. Arellano M & Bond S (1991) Some Tests of Specification for Panel Data - Monte-Carlo Evidence and an Application to Employment Equations. *Rev Econ Stud* 58(2):277-297.
19. Wild M, Ohmura A, & Makowski K (2007) Impact of global dimming and brightening on global warming. *Geophys Res Lett* 34(4).
20. Trenberth KE & Fasullo JT (2013) An apparent hiatus in global warming? *Earth's Future* 1(1):19-32.
21. Meehl GA, Arblaster JM, Fasullo JT, Hu AX, & Trenberth KE (2011) Model-based evidence of deep-ocean heat uptake during surface-temperature hiatus periods. *Nature Climate Change* 1(7):360-364.
22. Santer BD*, et al.* (2014) Volcanic contribution to decadal changes in tropospheric temperature. *Nat Geosci* 7(3):185-189.
23. Skeie RB, Berntsen T, Aldrin M, Holden M, & Myhre G (2014) A lower and more constrained estimate of climate sensitivity using updated observations and detailed radiative forcing time series. *Earth Syst Dynam* 5(1):139-175.
24. Kosaka Y & Xie SP (2013) Recent global-warming hiatus tied to equatorial Pacific surface cooling. *Nature* 501(7467):403-+.
25. Klimont Z, Smith SJ, & Cofala J (2013) The last decade of global anthropogenic sulfur dioxide: 2000-2011 emissions. *Environ Res Lett* 8(1).
26. Smith SJ*, et al.* (2011) Anthropogenic sulfur dioxide emissions: 1850-2005. *Atmos Chem Phys* 11(3):1101-1116.